

Manuscript Details

Manuscript number	QUATINT_2017_195
Title	Evidence for a Younger Dryas deglaciation in the Galicica Mountains (FYROM) from cosmogenic ³⁶ Chlorine
Article type	Full Length Article

Abstract

This study presents the first cosmogenic ³⁶Cl surface exposure data from a moraine in the Former Yugoslav Republic of Macedonia (FYROM). Five limestone boulders from a terminal moraine in the Galicica Mountains (40.94°N, 20.83°E, 2050 m a.s.l.) were used for cosmogenic ³⁶Cl surface exposure dating. The ³⁶Cl concentrations from the five boulders are identical within their measurement uncertainties ruling out major effects of inheritance, erosion, or snow cover. The calculated ages are very consistent ranging from 11.3 to 12.8 ka (mean 12 ka) after applying a Ca-spallation production rate of 56 at g⁻¹ a⁻¹ (LSD scaling) and correction for 5 mm ka⁻¹ carbonate weathering and 2 % snow shielding. The applied corrections for weathering and snow shielding cause a shift to older ages in the order of magnitude of ca. 5 % on average, making the production rate the main impact on exposure ages. The ages point to a moraine formation during the Younger Dryas period, consistent with the timing of the last deglaciation in the Galicica Mountains derived from previous geomorphological studies in the area. The formation of a glacier was likely favoured by several topoclimatic factors, accounting for additional snow input. This interpretation is in line with regional studies on glaciation chronologies from Šara Range (FYROM/Republic of Kosovo), Retezat Mountains (Romania), Mount Orjen (Montenegro) and Durmitor (Montenegro). Lake sediment analyses of lakes Prespa (Republic of Albania/FYROM/Greece), Maliq (Republic of Albania) and Dojran (FYROM/Greece) indicate that cold conditions promoted the formation of a local cirque glacier. However, studies of sediment records of the adjacent lakes Ohrid (Republic of Albania/FYROM) and Prespa do not indicate the presence of a proximal glaciation. An explanation might be a combination of the small size of the cirque glacier, generating only small amounts of debris, and the karstic bedrock, which hampers fluvial transport and acts by its aquifer system as a natural sediment trap, as the fluvial transport of the sediments to the lakes is absorbed by the karst system.

Keywords	Galicica Mountains; Chlorine-36 (³⁶ Cl); Cosmogenic surface exposure dating; Younger Dryas; Balkan Peninsula; Moraine
Corresponding Author	Raphael Gromig
Corresponding Author's Institution	Institute of Geology and Mineralogy, University of Cologne
Order of Authors	Raphael Gromig, Silke Mechernich, Adriano Ribolini, Bernd Wagner, Giovanni Zanchetta, Ilaria Isola, monica bini, Tibor Dunai
Suggested reviewers	Susan Ivy-Ochs, Mehmet Akif Sarıkaya, Philip. Hughes

Submission Files Included in this PDF

File Name [File Type]

cover_letter_gromig.pdf [Cover Letter]

Author_agreement_form.pdf [Author Agreement Form]

Manuscript_gromig_et al.docx [Manuscript]

FIG1PDF.pdf [Figure]

FIG2TIFF.tif [Figure]

FIG3JPEG.jpg [Figure]

FIG4PDF.pdf [Figure]

FIG5PDF.pdf [Figure]

FIG6TIFF.tif [Figure]

To view all the submission files, including those not included in the PDF, click on the manuscript title on your EVISE Homepage, then click 'Download zip file'.



Universität zu Köln • Zülpicher Straße 49a • 50674 Köln

To the editor of
Quaternary International

**Mathematisch-
Naturwissenschaftliche
Fakultät**

**Institut für Geologie und
Mineralogie**

M.Sc. Geow. Raphael Gromig

Telefon +49 221 470-6478
Telefax +49 221 470-1663

gromigr@uni-koeln.de
www.uni-koeln.de/math-nat-fak/geomin/

To whom it may concern,

We conducted a study in the Galicica Mountains (Former Yugoslav Republic of Macedonia) on a terminal moraine of Younger Dryas age using cosmogenic ³⁶Chlorine surface exposure dating. The data has been set in context to other Balkan deglaciation chronologies. Also paleoclimate reconstructions derived from nearby lake records were evaluated concerning a possible imprint of a local glaciation on the sedimentation pattern of the lake on the one hand, and if the climate reconstructions reveal favourable climate during the time of a local glaciation on the other hand.

Köln den 21.02.17

We are confident that Quaternary International would be an excellent journal to publish this data since it would stand in line with similar publications (e.g. Reuther et al., 2007, Makos et al., 2013, Kuhlemann et al., 2013). This study contributes to the reconstruction of glaciations on the Balkan Peninsula.

Thank you in advance for considering to publish our research.

Best regards


Raphael Gromig



Quaternary International

We the authors declare that this manuscript is original, has not been published before and is not currently being considered for publication elsewhere.

We confirm that the manuscript has been read and approved by all named authors and that there are no other persons who satisfied the criteria for authorship but are not listed. We further confirm that the order of authors listed in the manuscript has been approved by all of us.

We understand that the Corresponding Author is the sole contact for the Editorial process. He/She is responsible for communicating with the other authors about progress, submissions of revisions and final approval of proofs.

Sincerely,

On behalf of all authors

A handwritten signature in black ink, consisting of a stylized initial 'R' followed by a long, sweeping horizontal line that loops back under itself.

1 **Evidence for a Younger Dryas deglaciation in the Galicica Mountains (FYROM) from**
2 **cosmogenic ³⁶Chlorine**

3

4 Raphael Gromig^a, Silke Mechernich^a, Adriano Ribolini^b, Bernd Wagner^a, Giovanni
5 Zanchetta^b, Ilaria Isola^c, Monica Bini^b, Tibor J. Dunai,^a

6 ^aInstitute of Geology and Mineralogy, University of Cologne, Zulpicher Str. 49a, 50674
7 Cologne, Germany

8 ^bDipartimento di Scienze della Terra, University of Pisa, via S. Maria 53, 56126 Pisa, Italy

9 ^cIstituto Nazionale di Geofisica e Vulcanologia, Via della Faggiola 32, 56126 Pisa, Italy

10 Corresponding author: Raphael Gromig. Email contact: gromigr@uni-koeln.de Phone: +49
11 (0)221 470 6478

12

13 **Abstract**

14

15 This study presents the first cosmogenic ^{36}Cl surface exposure data from a moraine in the
16 Former Yugoslav Republic of Macedonia (FYROM). Five limestone boulders from a terminal
17 moraine in the Galicica Mountains (40.94°N, 20.83°E, 2050 m a.s.l.) were used for
18 cosmogenic ^{36}Cl surface exposure dating. The ^{36}Cl concentrations from the five boulders are
19 identical within their measurement uncertainties ruling out major effects of inheritance,
20 erosion, or snow cover. The calculated ages are very consistent ranging from 11.3 to 12.8 ka
21 (mean 12 ka) after applying a Ca-spallation production rate of 56 at $\text{g}^{-1} \text{a}^{-1}$ (LSD scaling) and
22 correction for 5 mm ka^{-1} carbonate weathering and 2 % snow shielding. The applied
23 corrections for weathering and snow shielding cause a shift to older ages in the order of
24 magnitude of ca. 5 % on average, making the production rate the main impact on exposure
25 ages. The ages point to a moraine formation during the Younger Dryas period, consistent
26 with the timing of the last deglaciation in the Galicica Mountains derived from previous
27 geomorphological studies in the area. The formation of a glacier was likely favoured by
28 several topoclimatic factors, accounting for additional snow input. This interpretation is in line
29 with regional studies on glaciation chronologies from Šara Range (FYROM/Republic of
30 Kosovo), Retezat Mountains (Romania), Mount Orjen (Montenegro) and Durmitor
31 (Montenegro). Lake sediment analyses of lakes Prespa (Republic of
32 Albania/FYROM/Greece), Maliq (Republic of Albania) and Dojran (FYROM/Greece) indicate
33 that cold conditions promoted the formation of a local cirque glacier. However, studies of
34 sediment records of the adjacent lakes Ohrid (Republic of Albania/FYROM) and Prespa do
35 not indicate the presence of a proximal glaciation. An explanation might be a combination of
36 the small size of the cirque glacier, generating only small amounts of debris, and the karstic
37 bedrock, which hampers fluvial transport and acts by its aquifer system as a natural sediment
38 trap, as the fluvial transport of the sediments to the lakes is absorbed by the karst system.

39

40 **Keywords:** Galicica Mountains, Chlorine-36 (^{36}Cl), Cosmogenic surface exposure dating,
41 Younger Dryas, Balkan Peninsula, Moraine

42

43

44 **1 Introduction**

45 The glaciation history on the Balkan Peninsula is subject of research since the late 19th
46 century (Hughes et al., 2011 and references therein). It is of particular interest since glacier
47 reconstructions provide a valuable tool to contribute to Quaternary paleoclimate
48 reconstructions. The southerly latitude position of these former glaciers on the Balkan
49 Peninsula made them especially sensitive to climatic changes, i.e. they react faster with
50 glacier retreat or advance if there are even minor shifts in the climatic conditions (Hughes
51 and Woodward, 2008; Sarikaya et al., 2014). Several glaciations occurred and are
52 documented on the Balkan Peninsula since the Mid Pleistocene. To date, numerous glacial
53 studies in the Balkan Mountains have been carried out, for example in the Durmitor Massif,
54 Mount Orjen and Mount Lovćen in Montenegro (Hughes, 2010; Hughes et al., 2011; Žebre
55 and Stepišnik, 2014), Mount Prokletije in the Albanian Alps (e.g. Milivojević et al., 2008), the
56 Rila Mountains in Bulgaria (e.g. Kuhlemann et al., 2013), or Mount Tymphi and Mount
57 Smolikas in northern Greece (Hughes et al., 2003; Hughes et al., 2006a; 2007b, c.f. Fig. 6).
58 In most regions, the glaciation during the Marine Isotope Stage (MIS) 12 (Skarnellian Stage,
59 ca. 478 – 424 ka BP) (Lisiecki and Raymo, 2005) is considered to represent the maximum
60 glacier advances (e.g. Hughes et al., 2010; Hughes et al., 2011; Adamson et al., 2014).
61 However, a precise dating of glacial features, such as of moraines, is lacking in most studies.
62 One reason for the fragmentary age control is that many of the investigated areas are
63 composed of limestone, where age determination is limited to U-series dating of secondary
64 carbonate cements on moraines, which does not necessarily date the actual formation of a
65 moraine but the precipitation of the calcitic cement (Hughes et al., 2013). In some areas,
66 where quartz-bearing rocks are common, cosmogenic ¹⁰Be surface exposure dating was
67 conducted (e.g. Reuther et al., 2007; Kuhlemann et al., 2013).

68 Studies in the Former Yugoslav Republic of Macedonia (FYROM, in the following referred to
69 as Macedonia) are very rare, which is surprising, as Macedonia is situated in a central
70 position of the Balkan Peninsula. The Šara Mountain Range at the border of Macedonia and
71 the Republic of Kosovo was studied by Kuhlemann et al. (2009). In the Galicica Mountains,
72 which separate Lakes Ohrid and Prespa, a precise mapping of geomorphological features
73 allowed a reconstruction of the expansion of local cirque glaciers (Ribolini et al., 2011).

74 We now present the first cosmogenic ³⁶Cl exposure ages of a glacial moraine in the Galicica
75 Mountains. The results are set in context with the reconstructed deglaciation history of the
76 Balkan Peninsula in order to improve the understanding of the regional climate history. The
77 results are also compared to other sediment records from nearby lakes in order to test if the
78 results are in line with the paleoclimatic interpretation.

79
80
81

82 **2 Location, Regional Geology and Climate of the Galicica Mountains**

83 The Galicica Mountain Range is situated in the southern Balkan region (Fig. 1) and is mostly
84 belonging to the Republic of Macedonia. The highest peak is Magaro with a maximum
85 elevation of 2255 m above sea level (a.s.l.). The mountain range is framed by the Ohrid
86 graben with Lake Ohrid (693 m a.s.l.) to the west and the Prespa graben with Lake Prespa
87 (849 m a.s.l.) to the east. Towards the south, the Galicica Mountain Range extends into the
88 Republic of Albania, where it is named Mali i Thatë Mountains, with the highest peak being
89 Kota with an elevation of 2265 m a.s.l. (Watzin et al., 2002; Bordon et al., 2009; Hoffmann et
90 al., 2010).

91

92 The Galicica Mountains are a horst structure, which is intersected by a E-W striking normal
93 fault, creating a wind gap extending from Lake Prespa to Ohrid (Hoffmann et al., 2010). The
94 Galicica Mountains are mainly composed of Triassic and subordinated Early Jurassic
95 (Hoffmann et al., 2010) unfossiliferous limestones and locally dolomites (Wagner et al., 2008;
96 Ribolini et al., 2011). The limestones are strongly karstified, rugged and broken (Wagner et
97 al., 2008). Isolated clastic sedimentary rocks of Triassic age occur occasionally (Vogel et al.,
98 2010b). However, the area studied here in more detail, located ca. 2 km south of the wind
99 gap (Fig. 1, further described below) is entirely composed of Triassic limestone. The cirque is
100 approx. 400 m wide. The headwall is partly very steep, producing large slope debris
101 surfaces. Rockfalls, generating large boulders debris, are also active today, forming a belt of
102 large blocks at the base of talus fan (Ribolini et al., 2011).

103

104 The large scale climate in Macedonia is controlled by the proximity to the Aegean Sea in the
105 south-east and the Adriatic Sea in the west. Additionally, the surrounding mountains have a
106 crucial influence on the regional climate, which shows characteristics of Mediterranean as
107 well as continental influences (Watzin et al., 2002; Leng et al., 2013). At higher altitudes,
108 montane climate predominates, with higher daily temperature differences compared to the
109 areas in close proximity of lakes Ohrid and Prespa, that buffer daily temperature variations
110 (Watzin et al., 2002). The climate at lakes Ohrid and Prespa for the period between 1961 and
111 1990 is recorded by several weather stations at altitudes below 1020 m a.s.l.. Present day
112 weather stations at higher altitudes unfortunately do not exist. The Ohrid meteorological
113 station (760 m a.s.l., near the city of Ohrid) recorded an annual average temperature of 11.1°
114 C, whereas Resen meteorological station (881 m a.s.l.) at Lake Prespa recorded a mean
115 annual temperature of 9.5°C (Popovska and Bonacci, 2007). Applying a thermal lapse rate of
116 0.6 °C 100 m⁻¹ to the average annual temperature of Ohrid meteorological station leads to an
117 annual average temperature of ca. 3.4 °C at the altitude of the sampled moraine sequence,
118 which is situated at 2010 – 2050 m a.s.l. (ca. 2.5 °C based on the Prespa meteorological

119 station). The climate in the Lake Prespa watershed is considered to exhibit more temperature
120 variations compared to the Lake Ohrid watershed, as Lake Ohrid, which has a water volume
121 15 times larger than Lake Prespa, acts as a strong thermal buffer (Popovska and Bonacci,
122 2007). The precipitation data recorded between 1961 and 1990 reveals an annual average
123 precipitation of 907 mm in Lake Ohrid watershed and 795 mm in Lake Prespa watershed
124 (Popovska and Bonacci, 2007). After 1990 no continuous climate record is published.
125 Snowfall in the mountains is assumed to exceed 1 m annually and to last until late spring
126 (Hollis and Stevenson, 1997).

127 In total four moraine sequences were mapped in detail by Ribolini et al. (2011), and range in
128 altitudes from 1780 to 2050 m a.s.l. (Fig. 2). The studied moraine is located in the southern
129 of two cirques. The lower moraines (G1-3 sequences) are less well shaped and lack material
130 suitable for exposure dating. Ice moulted rocks occur and are partly covered by fluvio-glacial
131 deposits. Dating with other methods, i.e. radiocarbon dating, was also not possible, as a 4-m
132 deep borehole in the sediments dammed by the G3 moraine did not deliver datable material
133 and it was not possible to get deep enough, for a rough dating of the G3.

134 In contrast, at 2010 – 2060 m a.s.l. a series of well preserved nested moraines forms the G4-
135 moraine sequence (Fig. 2), which is considered to have built up in the course of the same
136 glaciation phase (Ribolini et al., 2011). The largest moraine ridge was sampled for
137 cosmogenic ^{36}Cl dating on carbonates (Fig. 3). The distance of the G4 moraine to the
138 headwall of the cirque is approx. 400 m and thus most likely not affected by rockfalls from the
139 headwall, also due to the elevated position. The moraine is mainly composed of limestone
140 blocks, pebbles and coarse gravel. Depressions between the ridges originated from glacier
141 retreat stages. Karst dissolution and permafrost creep may have intensified deformation of
142 the original topography of some ridges (Ribolini et al., 2011).

143

144 **3 ^{36}Cl dating method**

145 ^{36}Cl dating has successfully been applied to reconstruct glacial chronologies in several
146 areas (e.g. Phillips et al., 1997; Makos et al., 2013; Sarıkaya et al., 2014).

147 With known production rates, the built up of cosmogenic nuclides can be converted into
148 ages, which reflects the time, when the dated material was first exposed to secondary
149 cosmic rays. For this application, the surface exposure ages mark the point of a glacier
150 retreat when fresh rock is deposited in terminal moraines, which then start to accumulate
151 cosmogenic nuclides.

152

153 *3.1 Sample collection*

154 Five limestone boulders in or near crest-position of the well-defined terminal moraine G4
155 were sampled for ^{36}Cl exposure dating (Fig. 3). Today, the moraine exhibits a crest height of

156 approx. 14 m with reference to the base of the uphill side of the moraine and shows
157 implications of only moderate degradation since deposition. Boulders were chosen based on
158 their size, their plausibility to be in stable position and their post-depositional preservation.
159 The samples themselves were collected at the upper surfaces of each boulder with a hammer
160 and chisel (Fig. 4). Horizon angles were measured in the field using an inclinometer in 20°
161 intervals in order to correct for topographic shielding.

162

163 3.2. *Sample preparation*

164 The samples were treated mechanically and chemically at the laboratory facilities of the
165 Institute of Geology and Mineralogy at the University of Cologne, Germany, following mainly
166 the chemistry protocol of (Stone et al., 1996). The weathered rock surface and any
167 contaminations like recrystallized calcite or lichen were mechanically removed using a hand
168 held rotary tool with a diamond bit. This is relevant as they can contain a relevant amount
169 ³⁵Cl, which acts as a target element to produce ³⁶Cl by thermal neutrons. Subsequently, the
170 boulders were crushed and sieved and the 250 – 500 µm grain size fraction was treated with
171 30 % H₂O₂ at 40° C for 96 hours in order to remove any residual organic matter. Each aliquot
172 was rinsed and leached twice in 0.3 M HNO₃ until ~13% of material was removed in order to
173 eliminate any meteoric ³⁶Cl. Afterwards the samples were spiked with a known amount of
174 isotopically enriched stable chloride carrier to allow simultaneous determination of the natural
175 chlorine and ³⁶Cl (Desilets et al., 2006 and references therein). After adding the carrier and
176 some excess AgNO₃ to avoid degassing, ~22 g of each sample were dissolved using MilliQ
177 water and subsequent careful addition of 2 M HNO₃. As sulphur displays a major issue for
178 Accelerator Mass Spectrometer (AMS) ³⁶Cl measurement, because ³⁶S it is an isobar of ³⁶Cl,
179 it was removed by extraction of crystallized BaSO₄ after addition of Ba(NO₃)₂. Finally, the
180 precipitated and dried AgCl powder was pressed into AMS cathodes and measured at the
181 CologneAMS facility (Klein et al., 2011). To track any chlorine contamination in the chemistry
182 process, a chemistry blank is coupled with each series and measured in the same AMS run.

183

184 3.3. *Sample Measurements (AMS; Actlabs, ICP-OES)*

185 To ensure the accuracy and precision of the AMS measurement, the AMS was calibrated
186 and normalized to three standards with different concentrations (³⁶Cl/Cl: 5.000 x 10⁻¹³, 1.600
187 x 10⁻¹², and 1.000 x 10⁻¹¹) from the NIST SRM 4843 material (Sharma et al., 1990).
188 Additionally, we prepared four pure spike blanks (Oak Ridge National Laboratory batch
189 150301, NaCl enriched with ³⁵Cl), and five blanks with the ³⁵Cl/³⁷Cl natural ratio of 3.127 (four
190 Standard Reference Material 975 and a commercial NaCl purchased from VWR company).

191 Major and trace element contents of bulk non-leached sample material were measured by
192 fusion inductively coupled plasma and fusion mass spectrometry at Actlabs, Canada (Table

193 1), in order to calculate the sample specific production rate of ^{36}Cl . These analyses were only
194 performed for RG14/001 and RG14/005 since the limestone is very homogeneous, the
195 catchment is small and the natural chlorine content of the sample is very low. The
196 measurement of the two samples, therefore, can be considered as representative. In
197 addition, an aliquot of each dissolved sample was analyzed on the ICP-OES at the Institute
198 of Geology and Mineralogy in Cologne to reveal the composition of the target AMS-
199 measured fraction (Table 1). The concentration of ^{36}Cl and natural chlorine was measured
200 via AMS at the CologneAMS facility (Table 2).

201

202 **4 Results**

203 *4.1 Sample chemistry*

204 Major as well as minor element concentrations point to a relatively pure limestone (Table 1).
205 For samples RG14/002, RG14/003 and RG14/004, values from the measurement of
206 RG14/001 were taken. Applying the value of RG14/005 instead of RG14/001 was tested and
207 the effect was minor i.e. in the range of ca. 1%. Elements, which can have a crucial influence
208 on the formation of ^{36}Cl via the thermal neutron pathway are consistently very low. Also K, Fe
209 and Ti, on which ^{36}Cl can be produced spallogenically, are low. Radiogenic production of ^{36}Cl
210 can also be excluded, as Uranium and Thorium, which can act as a neutron source once
211 they decay (Bierman et al., 1995), were below detection limit in the sampled rocks.

212

213 **Table 1: Chemical composition of samples. Values below detection limit are marked with “<”.**

Sample ID	Major elements											Trace elements					
	SiO2 (wt-%)	TiO2 (wt-%)	Al2O3 (wt-%)	Fe2O3 (wt-%)	MnO (wt-%)	MgO (wt-%)	CaO (wt-%)	Na2O (wt-%)	K2O (wt-%)	P2O5 (wt-%)	CO2 (LOI) (wt-%)	Cl ppm	B ppm	Sm ppm	Gd ppm	U ppm	Th ppm
RG14/001 - 004	0.71	0.003	0.28	0.04	0.003	0.4	54.92	0.09	0.05	0.03	42.56	23.6	< 0.5	<0.1	0.1	0.3	0.2
RG14/005	0.19	0.01	0.5	0.04	0	0.48	53.29	0	0	0.02	40.02	35.2	30	0.1	< 0.1	0.1	< 0.1

215

216 *4.2 Cl and ³⁶Cl concentrations*

217 Stable chlorine concentrations of the samples are consistently low ranging from 16 ± 1 to 34
218 $\pm 2 \mu\text{g g}^{-1}$, indicating that the thermal neutron production of ³⁶Cl has only a minor contribution
219 to the total production. Blank corrections were obtained from subtracting the number of Cl
220 and ³⁶Cl atoms in the blank from the respective atoms in the samples, which resulted in a
221 decrease of the uncorrected ³⁶Cl concentration by 1.2 - 1.4%. The measured ³⁶Cl
222 concentrations are very consistent, ranging from $1.07(10^6)$ at g^{-1} to $1.21(10^6)$ at g^{-1} . This
223 reflects a high precision of the measurement and a low geological variability (Table 2).

224

225 **Table 2: Sample specific characteristics. A bulk density of 2.6 g cm⁻³ is assumed for all samples.**

226

Sample ID	Latitude	Longitude	Altitude	thickness of sample	Topographic shielding factor	³⁶ Cl conc. (atoms g ⁻¹)	³⁵ Cl/ ³⁷ Cl	³⁶ Cl/ ³⁷ Cl	Prod. Rate (atoms g ⁻¹ a ⁻¹)	calc. Age [°] with 0 mm ka ⁻¹ erosion	calc. Age* with 5 mm ka ⁻¹ erosion	calc. Age [°] with 10 mm ka ⁻¹ erosion	calc. Age [°] with 5 mm ka ⁻¹ erosion
	°N (DD)	°E (DD)	m.a.s.l.	cm									
RG 14/001	40.937333	20.825389	2051	2	0.964	1.07E+06	9.231	6.981E-12	86.26	10.75 ± 1.11	11.28 ± 1.28	11.39 ± 1.39	10.78 ± 1.21
RG 14/002	40.937417	20.825472	2050	3	0.964	1.19E+06	7.726	6.015E-12	87.83	11.77 ± 1.08	12.25 ± 1.17	11.32 ± 1.26	11.79 ± 1.20
RG 14/003	40.937583	20.825500	2048	2	0.964	1.13E+06	8.239	6.4E-12	87.28	11.24 ± 1.18	11.74 ± 1.23	11.81 ± 1.08	11.26 ± 1.09
RG 14/004	40.937694	20.825361	2040	2	0.967	1.10E+06	10.555	9.138E-12	84.80	11.26 ± 1.13	11.90 ± 1.29	12.09 ± 1.41	11.30 ± 1.29
RG 14/005	40.937889	20.825056	2048	6	0.969	1.21E+06	7.623	6.151E-12	86.29	12.18 ± 1.23	12.79 ± 1.42	13.01 ± 1.31	12.21 ± 1.06
Blank B3	-	-	-	-	-		19.452	2.70E-13		-	-	-	-

227 ^ total sample specific contemporary depth average production rate

228 * corrected for snow shielding (2%)

229 ° no snow correction applied

230 4.3 ³⁶Cl ages

231 Exposure ages of the sampled boulders were computed based on the measured Cl isotope
232 ratios. For the calculations, we used cosmogenic ³⁶Cl production rates of 56 ± 4.1 at ³⁶Cl(g
233 Ca)⁻¹ a⁻¹ for Ca spallation (Marrero et al., 2016), which is the main production pathway,
234 accounting for ca. 90-94 % of ³⁶Cl production. K spallation production rates of 155 ± 11 at
235 ³⁶Cl (g K)⁻¹ yr⁻¹ (Marrero et al., 2016) were used, but the impact of this production pathway is
236 low due to the low K content in the samples. Used thermal neutron production rate is $759 \pm$
237 180 neutrons (g air)⁻¹ a⁻¹ (Marrero et al., 2016). Also production via thermal neutron capture
238 is minor as the stable Cl content of the samples is low (Table 2), ranging from ca. 5-7.5 %.
239 Production of ³⁶Cl via muons is also subordinated, accounting for ca. 2.5 % of the total
240 production. These production rates are scaled to sea level and high geomagnetic latitude. In
241 order to account for site-specific variations in the atmospheric secondary cosmic-ray flux
242 scaling factors of Lifton et al. (2014) were applied. The surface exposure ages were
243 calculated from the measured ³⁶Cl concentrations using the CRONUScalc (Cosmic-Ray
244 Produced Nuclide Systematics on Earth) (accessed October 2016) calculator with the
245 software Matlab® (R2016a, MathWorks®). The calculation allows for corrections for e.g.
246 shielding, which can be due to topographic shielding and snow cover, and erosion.
247 Topographic shielding correction factors as well as the sample-specific attenuation length
248 were determined using the CRONUS calculator. The exposure ages range between 10.8 ka
249 and 12.2 ka, with a mean age of 11.4 ka and a median of 11.3 ka (Table 2) without
250 corrections for erosion and no snow shielding and using of 56 ± 4.1 at ³⁶Cl(g Ca)⁻¹ a⁻¹ for
251 spallation. Correction factors are individually discussed in chapter 5.1.

252

253 5 Discussion

254 5.1 ³⁶Cl age calculation uncertainties

255 The results of the timing of the moraine formation depend on different input parameters used
256 for the age calculations, such as erosion, snow shielding, inheritance, and production rates.
257 A proper discussion of these input parameters is needed to evaluate the robustness of the
258 dating results. Major corrections and assumptions were defined by the following aspects:

259 (i) **Erosion:** Field observations did not indicate significant erosion of the upper boulder
260 surfaces itself (especially chemical weathering due to dissolution of limestone). However,
261 below the G4 moraine series, limestone surfaces exhibit weathering channels carving
262 several centimeters deep into the rock surface, suggesting dissolution of carbonatic rock
263 surfaces due to precipitation. Chemical weathering of limestone can cause erosion rates of
264 up to 10 mm ka⁻¹, according to observations of Ivy-Ochs et al. (2009). A dissolution rate in
265 this magnitude is in accordance with field experiments of (Plan, 2005). Experiments with
266 micro-erosion meters also confirm limestone dissolution rates in the same order of

267 magnitude or even higher (Stephenson and Finlayson, 2009 and references therein). We
268 think that 10 mm ka^{-1} represents a maximum possible erosion rate. However, we propose a
269 lower erosion rate/limestone dissolution rate of 5 mm ka^{-1} since field observations do not
270 suggest any higher limestone dissolution rates on the boulders itself.

271 (ii) **Snow Shielding:** The combination of Mediterranean as well as continental climate in the
272 region (Watzin et al., 2002), leads to substantial snow cover in the Galicica Mountains in
273 winter (Hollis and Stevenson, 1997). Hence, ignoring the effect of snow could lead to an
274 underestimation of the surface exposure ages. Correction for snow shielding is difficult to
275 assess for several reasons:

- 276 i) Climate data from locations with similar altitudes as the sampling site are not
277 available
- 278 ii) Climatic conditions likely changed throughout the Holocene
- 279 iii) The effect of elevation of boulders on moraine crest is unclear
- 280 iv) Topography-related effects on snow accumulation unclear
- 281 v) The effect of snow shielding is not completely understood yet

282 A potential reduction of the production of the target element due to snow cover (Gosse and
283 Phillips, 2001) was partly disproved by Dunai et al. (2014). A hydrogen rich cover, such as
284 from snow, can significantly increase the production rate of certain nuclides (e.g. ^{36}Cl).
285 However, since the concentration of ^{35}Cl is consistently low throughout all five samples, the
286 reinforcing effect of a snow cover is very limited. Hence, we assume that snow cover has a
287 net attenuating effect of the production of ^{36}Cl . Based on the available literature (Hollis and
288 Stevenson, 1997), we suggest a snow cover of 0.3 m for an average duration of 4 months
289 per year with a density of $0.3 \text{ g (cm}^3\text{)}^{-1}$, leading to an age correction of approx. 2%, using the
290 equation of Gosse and Phillips (2001).

291 (iii) **Inheritance:** The exposure ages are very consistent with only minor differences within
292 the analytical uncertainties of the ^{36}Cl concentrations. The present debris fans indicate a high
293 supply of new rock material, which leads to a continuous renewal of the cliff surface.
294 According to Putkonen and Swanson (2003) the chance of dating boulders with significant
295 prior exposure is extremely low in settings, where erosion at the source rock delivering rock
296 debris is high. Relatively high temperature differences between day and night cycles as well
297 as frost shattering during winter season might be the driving mechanisms for relatively high
298 physical weathering. Inheritance can thus be ruled out.

299 (iv) **Production rates:** The amount of studies determining ^{36}Cl production rates is still limited
300 and the published rates scatter significantly, particularly for Ca spallation and the muonic
301 contribution. We used production rates recently published by Marrero et al. (2016) for which
302 one out of three calibrations sites are on the same latitude as our study site and the
303 published production rates are scaled to scaling factors of Lifton et al. (2014), to calculate the

304 exposure ages. Since the geographical position of the Galicica Mountains is very close to the
305 sampling sites for production rate studies of Schimmelpfennig et al. (2011), we also tested
306 these production rates, which are in the order of ca. 20-25 % lower for Ca spallation and ca.
307 2-17 % for K spallation (depending on scaling model, respectively) than those of Marrero et
308 al. (2016), respectively, in order to calculate ages.

309

310 The uncorrected ages (Table 2) can be regarded as minimum ages. Applying an erosion rate
311 of 5 mm ka⁻¹ does not have any significant impact on the ages but should also not be ignored
312 (Fig. 5). An applied erosion of 10 mm ka⁻¹ shows a more significant effect towards older ages
313 in the order of 0.5 - 0.8 ka. We do not suggest that such a relatively high erosion rate applies
314 to the sampled boulders in this particular geological setting, we rather want to illustrate, that
315 erosion as one of the major correction factors has only a minor influence in such young
316 samples. The incorporation of snow shielding (2%) has an impact on the ages to the same
317 degree than the applied maximum erosion rate. In contrast to erosion and snow shielding,
318 the selection of Ca spallation production rates plays a crucial role regarding the impact on
319 the surface exposure ages. Applying the Ca spallation production rate of Schimmelpfennig et
320 al. (2011) yields significantly older ages, ranging from 13.9 to 15.5 ka (uncorrected for
321 erosion). These ages are consistently younger than the time frame assessed for the global
322 last glacial maximum (LGM, 26.5 ka to 19 ka, Clark et al., 2009), even when applying an
323 erosion rate of 10 mm ka⁻¹ and consequently, a moraine formation in the course of a
324 deglaciation after the LGM can be excluded. These ages, however, would correspond to the
325 Older Dryas period, but as a consequence, no evidence for a Younger Dryas moraine would
326 then be evident. We favour the recently determined Ca spallation rate of Marrero et al.
327 (2016) and think that the Ca spallation rate of Schimmelpfennig et al. (2011) indicate
328 maximum ages and rather overestimate the surface exposure ages.

329 In this study because the ³⁶Cl concentrations and the calculated ages cluster very closely, we
330 can rule out a significant impact of moraine degradation and assume a permanent exposition
331 of the boulders, which reflect the actual deposition of the moraine. Consequently, only
332 chemical weathering due to precipitation needs to be taken in to account. Hence, the
333 calculated ages range from 11.3 to 12.8 ka (mean 12 ka) after correction for 5 mm ka⁻¹
334 erosion, snow cover and topographic shielding. In this case the glacier advance forming this
335 moraine was centered in the Younger Dryas cold period. The sampled moraine is part of a
336 series of nested moraines located in the cirque. Taking the stratigraphical order into account
337 the sampled moraine is the second oldest one of the G4 moraine sequence. Thus, the
338 moraine likely represents a stage of the glacier stagnation after the maximum advance has
339 already occurred.

340

341 *5.2 Galicica moraine ages*

342 Since the dated moraine is only one part of the G4 moraine series, the deglaciation after the
343 Younger Dryas glacier advance was likely interrupted by stagnations, leading to the
344 multicrested shape of the G4 moraine series.

345 Assuming that the G4 moraine sequence was formed in the course of the Younger Dryas
346 period, the G3 moraine, which is situated on an altitude of ca. 1930 m a.s.l. was likely formed
347 at either the Oldest Dryas period (ca. 17.5 – 14.5 ka BP), LGM or MIS 6 (ca. 190 – 130 ka
348 BP). Also a moraine formation at the Older Dryas can be possible. Moreover it can be stated,
349 that no glacier advances during the entire Holocene took place, due to a lack of
350 geomorphological evidence.

351

352 *5.3 Comparison to glaciation timing of other Balkan Mountain Ranges*

353 Studies dating glacial retreats are very sparse on the Balkan Peninsula. However, findings in
354 other formerly glaciated areas are in good agreement with the results of this study. The most
355 proximal dated site to the Galicica Mountains is the Šara Range, which is situated at the
356 border of the Republic of Macedonia and the Republic of Kosovo. Kuhlemann et al. (2009)
357 sampled a series of moraines at altitudes between 1355 m a.s.l. and 2300 m a.s.l. for ¹⁰Be
358 surface exposure dating. The lowest moraine yielded ages of 19.4 ± 3.2 ka (1402 m a.s.l., N-
359 facing cirque) , 16.1 ± 2.3 and 12.4 ± 1.7 ka (1398 m a.s.l. and 1355 m a.s.l., respectively,
360 same moraine ridge, NE-facing cirque) and 14.4 ± 2.1 (1776 m a.s.l., S-facing cirque)
361 including corrections for erosion (10 mm ka^{-1}), respectively. The inconsistency of the ages is
362 explained by dislocation of some of the sampled boulders. However, the oldest age points to
363 a moraine formation in the course of the LGM, whereas the others could potentially represent
364 recessional moraines (Hughes et al., 2013). At higher altitudes (2020 – 2300 m a.s.l.)
365 moraines were ascribed to the Younger Dryas, with ages from 11.9 ± 1.7 to 14.7 ± 2.1 ka,
366 with the same corrections applied for erosion. The higher altitude of certain Younger Dryas
367 moraines compared to the G4 moraine is not surprising, since there is a precipitation
368 gradient on the Balkan Peninsula, which decreases from west to east (Kuhlemann et al.,
369 2009).

370 In the Retezat Mountains in Romania, Reuther et al. (2007) investigated glacial features and
371 dated N-facing moraines using cosmogenic ¹⁰Be for surface exposure dating. They identified
372 a Late Glacial glaciation phase clustering around 16.1 ± 0.5 ka, implying that the local LGM
373 was delayed by several thousand years compared to the global LGM, but coinciding with the
374 Oldest Dryas (Heinrich-event H1 ca. 16.8 ca ka BP). However, they also identified a moraine
375 ascribed to the Younger Dryas with ¹⁰Be ages of 11.4 ± 1.3 ka and 13.6 ± 1.5 ka (corrected
376 for 5 mm ka^{-1} erosion, uplift and snow cover). The boulders sampled for dating were not

377 deposited on the moraine ridge, but directly above and below the moraine, representing the
378 time frame of the moraine built-up, which is in good agreement with our results.

379 Kuhlemann et al. (2013) dated moraines in the Rila Mountains (Bulgaria) using cosmogenic
380 ^{10}Be . They identified two glacial stages during which moraines were formed. Similar as in the
381 Šara Mountains, the glacier retreats were asynchronous with the LGM, with moraines
382 dating at the beginning (24 – 23 ka BP) and the termination of the LGM (18 – 16 ka BP).
383 Moraines documenting a glacier retreat at the Oldest Dryas and the Younger Dryas are not
384 dated but suggested based on stratigraphical relationship of geomorphological findings,
385 respectively.

386 A number of studies exist from Montenegro. Studies of Hughes et al. (2010) on Mt. Orjen
387 revealed the presence of Younger Dryas moraines based on U-Series dating of secondary
388 carbonates in moraines. These moraines are situated approx. 500 m lower than the G4
389 moraine in the Galicica Mountains. The differences in altitudes can be due to different local
390 topoclimatic factors and much higher precipitation in Montenegro (today ca. 5000 – 6000 mm
391 a^{-1}), which may have led to a much thicker snow cover and a lower equilibrium line altitude
392 (ELA).

393 Also for the Durmitor Massif in Montenegro Younger Dryas moraines are reported by Hughes
394 et al. (2011). Hughes et al. (2006a, 2007b) argue that maximum glacier advances in the
395 Pindus mountains in Greece likely occurred between 30 and 25 ka, based on climate
396 modelling of the pollen record of Lake Ioannina, which would be in agreement with the
397 assumption of Kuhlemann et al. (2013) of dryness during the LGM. However, also evidence
398 for a glacier readvance is reported for the Pindus Mountains (Hughes et al., 2006b).

399 For Mt. Prokletije at the border to Albania, Milivojević et al. (2008) hypothesize, based on
400 detailed geomorphological mapping, calculation of ELAs and comparison of those to other
401 Mediterranean mountains that the last of a total of three glacier advances occurred during
402 the Younger Dryas. At Mount Lovćen moraine sequences are believed to be of older origin
403 than Younger Dryas, most likely of LGM age (Žebre and Stepišnik, 2014). Precise correlation
404 is not possible due to a lack of a dating of the geomorphological evidence.

405 The lack of evidence for Younger Dryas glaciation in certain areas might have different
406 causes. Topoclimatic factors, such as regional temperature and precipitation can play a key
407 role for the formation of a glacier. Additional snow availability can be promoted by
408 avalanching, and wind blown snow into a cirque. The latter is likely in the Galicica Mountain
409 range from the plateau topping the cirque. Hughes (2009) proposes that avalanching in front
410 of steep cliffs and snow drift can increase the snow accumulation by a factor of two as shown
411 for present day glaciers at Mount Prokletije (Albania/Montenegro). Moreover, the orientation
412 of the cirque can promote glacier activity. A N-E oriented cirque enables a better shading,
413 which can lead to less ablation due to direct solar radiation (Evans, 1977; Hughes et al.,

414 2006a). This feature is in particular common for glaciations younger than MIS 12 (Hughes et
415 al., 2007a). Also the geology may play a significant role in glacier formation. In the Galicica
416 Mountains, the karstic bedrock may have led to a formation of initial depressions, which then
417 acted as a snow-trap and promoted the accumulation of snow. Also the relatively light color
418 of limestone and, hence, relatively high albedo may have set favourable conditions for a
419 glacier growth (Hughes et al., 2006a). Taken together, these factors can explain the
420 formation of a glacier due to only a modest increase of the local ELA, which was calculated
421 to 2130 m a.s.l with respect to the ELA for the G2-3 glacial phase, (calculated to ca. 2000 m
422 a.s.l.) (Ribolini et al., 2011). This is significantly lower than the calculated ELA (2300 m a.s.l.)
423 for the Šara Mountain range for the Younger Dryas.(Kuhlemann et al., 2009).

424

425 *5.4 The Younger Dryas in the sedimentary records of lakes Ohrid, Prespa, Maliq, and Dojran*

426 It is likely that the dated moraine was formed during a more windy or wet period of the
427 Younger Dryas.

428 Nearby paleoclimate records reveal a sharp transition from the relatively warm and humid
429 Bølling/Allerød interstadial to the Younger Dryas period (Bordon et al., 2009; Lézine et al.,
430 2010; Panagiotopoulos et al., 2013). Adrop of the mean annual temperature of around 10°C
431 is reconstructed at Lake Maliq (Bordon et al., 2009), and lakes Ohrid and Prespa record (Fig.
432 1) the last occurrence of ice rafted debris during the Younger Dryas (Vogel et al., 2010a;
433 Aufgebauer et al., 2012). However, the Younger Dryas does not seem to have had constant
434 cold and dry conditions. Bordon et al. (2009) subdivide the Younger Dryas into three periods
435 according to best modern analogue technique using pollen assemblages: whilst 12.8– 12.2
436 and 11.9 – 11.3 cal ka BP are interpreted as cold and dry, the intermediary interval was
437 slightly warmer and more humid. A paleoclimate record from Lake Prespa indicates rather
438 dry conditions between 13.2 and 12.6 cal ka BP, which were followed by wetter conditions
439 between 12.6 and 11.5 cal ka BP during the overall cold Younger Dryas (Aufgebauer et al.,
440 2012). This is in line with a shift in pollen assemblages, where a decrease in *Artemisia* and
441 *Chenopodiaceae* is correlated with an increase in tree taxa (Panagiotopoulos et al., 2013),
442 and with a shift in the diatom assemblages, which suggest increased moisture availability
443 after 12.3 ka BP (Cvetkoska et al., 2014). These findings are also in agreement with those
444 from Lake Dojran, located ca. 160 km to the east of the Galicica Mountains (Fig. 6). Lake
445 Dojran records an extreme lake level low-stand between 12.5 and 12.1 cal ka BP and a
446 subsequent higher lake level during the second part of the Younger Dryas period until 11.5
447 cal ka BP (Francke et al., 2013). The different climate conditions in the course of the
448 Younger Dryas are not recorded in Lake Ohrid, as its much larger water volume may have
449 buffered some climatic shifts. However, Vogel et al. (2010a) postulate enhanced aeolian
450 supply and a stronger wind activity during the Younger Dryas period in the surroundings of

451 Lake Ohrid, which potentially promote snow accumulation in the glacier cirque of the Galicica
452 Mountains.

453 Taking into account the errors of the respective age information for the lacustrine
454 successions as well as for the cosmogenic nuclides, an unambiguous alignment of the G4
455 moraine formation and the existence of a cirque glacier to one of the described more humid
456 periods during the Younger Dryas is not possible.

457

458 *5.5 Imprints of glacial erosion on lakes Ohrid and Prespa?*

459 Glacial activity usually enhances erosional processes that increase the amount of debris,
460 which is eventually transported into a sedimentary basin such as lakes Ohrid and Prespa.
461 Rather high supply of debris to the lakes would therefore be expected at the onset of the
462 deglaciation (Ballantyne, 2002) and would lead to an increase in the sedimentation rate of
463 both lakes during the Younger Dryas. However, the sediment cores from lakes Prespa
464 (Aufgebauer et al., 2012) and Ohrid (Vogel et al., 2010b) indicate relatively constant
465 sedimentation rates prior, during and after the Younger Dryas. Moreover, increased erosion
466 and transport from Galicica Mountain bedrock should increase the amount of detrital calcite
467 in the sediments of lakes Ohrid and Prespa. However, total inorganic carbon (TIC) is low
468 during the Younger Dryas and isotope investigations on the carbonates in the Lake Ohrid
469 sediments have revealed the formation of calcite is predominantly bound to authigenic
470 precipitation and siderite is formed diagenetically (Lacey et al., 2016).

471 The lack of a significant imprint of the reconstructed glaciation in the Galicica Mountains
472 during the Younger Dryas on the sediments of lakes Ohrid and Prespa might have three
473 different reasons. Firstly, the limited number of age control points constraining the time
474 period of the Younger Dryas in the sediment cores Co1202 (Ohrid) (Vogel et al., 2010a) and
475 Co1215 (Prespa) (Aufgebauer et al., 2012) is probably not sufficient to record variations in
476 the sedimentation rates on centennial time scales. Moreover, the regional geological setting
477 with the strongly karstified Galicica Mountain range may have buffered increased erosion
478 and sediment transport to the lakes. River runoff to lake Ohrid only accounts for ca. 25% of
479 the total inflow today (Wagner et al., 2010). Popovska and Bonacci (2007) report that 40 % of
480 the water discharging into Lake Ohrid at St. Naum at its south eastern shore close to the
481 investigated moraine is fed by karstic water derived from Lake Prespa. The remaining 60 %
482 of the inflow at St. Naum originate from direct precipitation over the Galicica Mountains,
483 which, however, drains directly into the karst system (Popovska and Bonacci, 2007). As a
484 result, only small rivers and creeks feed lakes Ohrid and Prespa today, and the majority of
485 water and sediments formed by the Galicica glacier may not have reached the lakes via
486 surficial pathways.

487 Similar processes were observed at Mount Orjen in Montenegro where glacier-derived
488 headwater became uncoupled from the depositional basin due to the formation of a
489 subterranean karst system (Adamson et al., 2014).

490 A third explanation for the lack of a significant change in the sedimentation patterns of the
491 lakes during the Younger Dryas is that the glacial erosion was relatively restricted. This
492 seems plausible taking the small distance between the slopes of the cirque and the dated
493 moraine, as well as the high distances to the shoreline of the recovered lacustrine sediment
494 successions in lakes Ohrid and Prespa.

495

496

497 **6 Conclusions**

498 Five boulders from a terminal moraine in the Galicica Mountains were dated using
499 cosmogenic ^{36}Cl surface exposure dating on limestones in Macedonia. The ages indicate a
500 moraine formation in the course of the Younger Dryas period based on surface exposure
501 ages centering at ca. 12 ka (corrected for 5 mm ka⁻¹ erosion and snow shielding).
502 Corrections for erosion and snow cover have only a minor effect on the age calculation. The
503 calculated exposure ages are in good agreement with several studies on deglaciation
504 chronology from the Balkan Peninsula. The timing of the formation of the glacier is in line
505 with sediment based paleoclimate reconstructions of the adjacent Lakes Prespa and Maliq
506 as well as Lake Dojran located ca. 160 km east of the Galicica Mountains, all of which point
507 to increased moisture availability along with cold temperatures and increased wind activity
508 from ca. 12.5 – 12.1 ka BP onwards.

509 On the other hand, the dated glacial event did not leave a significant imprint in the sediments
510 of the adjacent lakes Ohrid and Prespa, probably due to insufficient age control points to
511 constrain centennial variations in the sedimentation rates, the strong karstification of the
512 Galicica Mountains and decoupling of erosional transport from the sedimentary basins and
513 the restricted erosional force of the local glacier.

514 The results of this study display an important contribution to improve the glacial chronology
515 of the Balkan Peninsula and emphasize the necessity of analysing different archives of
516 paleoclimate information.

517

518 **7 Acknowledgements**

519 The fieldwork for this study was funded by the SCOPSCO (Scientific Collaboration On Past
520 Speciation Conditions in Lake Ohrid) project. We would like to thank Dr. Steven Binnie for
521 assistance with the chemical preparation of the samples in the cosmogenic nuclide
522 laboratory of the Institute of Geology and Mineralogy. We also are grateful to Dr. Karin
523 Boessenkool for assistance during the fieldwork. Dr. Alexander Francke is acknowledged for

524 valuable comments on the data of the sediment cores from Lake Ohrid and Lake Dojran.
525 Furthermore we would like to thank Dr. Shasta Marrero for very helpful advice for the
526 calculation of the ages with CRONUScalc.
527

528 **8 Bibliography**

- 529
530 Adamson, K.R., Woodward, J.C., Hughes, P.D., 2014. Glaciers and rivers: Pleistocene
531 uncoupling in a Mediterranean mountain karst. *Quaternary Science Reviews* 94, 28-43.
- 532 Aufgebauer, A., Panagiotopoulos, K., Wagner, B., Schaebitz, F., Viehberg, F.A., Vogel, H.,
533 Zanchetta, G., Sulpizio, R., Leng, M.J., Damaschke, M., 2012. Climate and environmental
534 change in the Balkans over the last 17 ka recorded in sediments from Lake Prespa
535 (Albania/F.Y.R. of Macedonia/Greece). *Quaternary International* 274, 122-135.
- 536 Ballantyne, C.K., 2002. A general model of paraglacial landscape response. *The Holocene*
537 12, 371-376.
- 538 Bierman, P., Gillespie, A., Caffee, M., Elmore, D., 1995. Estimating erosion rates and
539 exposure ages with ³⁶Cl produced by neutron activation. *Geochimica et Cosmochimica Acta*
540 59, 3779-3798.
- 541 Bordon, A., Peyron, O., Lézine, A.-M., Brewer, S., Fouache, E., 2009. Pollen-inferred Late-
542 Glacial and Holocene climate in southern Balkans (Lake Maliq). *Quaternary International*
543 200, 19-30.
- 544 Clark, P.U., Dyke, A.S., Shakun, J.D., Carlson, A.E., Clark, J., Wohlfarth, B., Mitrovica, J.X.,
545 Hostetler, S.W., McCabe, A.M., 2009. The Last Glacial Maximum. *Science* 325, 710-714.
- 546 Cvetkoska, A., Levkov, Z., Reed, J.M., Wagner, B., 2014. Late Glacial to Holocene climate
547 change and human impact in the Mediterranean: The last ca. 17 ka diatom record of Lake
548 Prespa (Macedonia/Albania/Greece). *Palaeogeography, Palaeoclimatology, Palaeoecology*
549 406, 22-32.
- 550 Desilets, D., Zreda, M., Almasi, P.F., Elmore, D., 2006. Determination of cosmogenic ³⁶Cl in
551 rocks by isotope dilution: innovations, validation and error propagation. *Chemical Geology*
552 233, 185-195.
- 553 Dunai, T.J., Binnie, S.A., Hein, A.S., Paling, S.M., 2014. The effects of a hydrogen-rich
554 ground cover on cosmogenic thermal neutrons: Implications for exposure dating. *Quaternary*
555 *Geochronology* 22, 183-191.
- 556 Evans, I.S., 1977. World-Wide Variations in the Direction and Concentration of Cirque and
557 Glacier Aspects. *Geografiska Annaler. Series A, Physical Geography* 59, 151-175.
- 558 Francke, A., Wagner, B., Leng, M.J., Rethemeyer, J., 2013. A Late Glacial to Holocene
559 record of environmental change from Lake Dojran (Macedonia, Greece). *Clim. Past* 9, 481-
560 498.
- 561 Gosse, J.C., Phillips, F.M., 2001. Terrestrial in situ cosmogenic nuclides: theory and
562 application. *Quaternary Science Reviews* 20, 1475-1560.
- 563 Hoffmann, N., Reichert, K., Fernández-Steeger, T., Grützner, C., 2010. Evolution of
564 ancient Lake Ohrid: a tectonic perspective. *Biogeosciences* 7, 3377-3386.
- 565 Hollis, G.E., Stevenson, A.C., 1997. The physical basis of the Lake Mikri Prespa systems:
566 geology, climate, hydrology and water quality. *Hydrobiologia* 351, 1-19.
- 567 Hughes, P.D., Gibbard, P.L., Woodward, J.C., 2003. Relict rock glaciers as indicators of
568 Mediterranean palaeoclimate during the Last Glacial Maximum (Late Würmian) in northwest
569 Greece. *Journal of Quaternary Science* 18, 431-440.
- 570 Hughes, P.D., Woodward, J.C., Gibbard, P.L., 2006a. Late Pleistocene glaciers and climate
571 in the Mediterranean. *Global and Planetary Change* 50, 83-98.
- 572 Hughes, P.D., Woodward, J.C., Gibbard, P.L., Macklin, M.G., Gilmour, M.A., Smith, G.R.,
573 2006b. The Glacial History of the Pindus Mountains, Greece. *The Journal of Geology* 114,
574 413-434.
- 575 Hughes, P.D., Gibbard, P.L., Woodward, J.C., 2007a. Geological controls on Pleistocene
576 glaciation and cirque form in Greece. *Geomorphology* 88, 242-253.
- 577 Hughes, P.D., Woodward, J.C., Gibbard, P.L., 2007b. Middle Pleistocene cold stage climates
578 in the Mediterranean: New evidence from the glacial record. *Earth and Planetary Science*
579 *Letters* 253, 50-56.
- 580 Hughes, P.D., Woodward, J.C., 2008. Timing of glaciation in the Mediterranean mountains
581 during the last cold stage. *Journal of Quaternary Science* 23, 575-588.
- 582 Hughes, P.D., 2009. Twenty-first Century Glaciers and Climate in the Prokletije Mountains,
583 Albania. *Arctic, Antarctic, and Alpine Research* 41, 455-459.

584 Hughes, P.D., 2010. Little Ice Age glaciers in the Balkans: low altitude glaciation enabled by
585 cooler temperatures and local topoclimatic controls. *Earth Surface Processes and Landforms*
586 35, 229-241.

587 Hughes, P.D., Woodward, J.C., van Calsteren, P.C., Thomas, L.E., Adamson, K.R., 2010.
588 Pleistocene ice caps on the coastal mountains of the Adriatic Sea. *Quaternary Science*
589 *Reviews* 29, 3690-3708.

590 Hughes, P.D., Woodward, J.C., van Calsteren, P.C., Thomas, L.E., 2011. The glacial history
591 of the Dinaric Alps, Montenegro. *Quaternary Science Reviews* 30, 3393-3412.

592 Hughes, P.D., Gibbard, P.L., Ehlers, J., 2013. Timing of glaciation during the last glacial
593 cycle: evaluating the concept of a global 'Last Glacial Maximum' (LGM). *Earth-Science*
594 *Reviews* 125, 171-198.

595 Ivy-Ochs, S., Poschinger, A.v., Synal, H.A., Maisch, M., 2009. Surface exposure dating of the
596 Flims landslide, Graubünden, Switzerland. *Geomorphology* 103, 104-112.

597 Klein, M.G., Dewald, A., Gott dang, A., Heinze, S., Mous, D.J.W., 2011. A new HVE 6MVAMS
598 system at the University of Cologne. *Nuclear Instruments and Methods in Physics Research*
599 *Section B: Beam Interactions with Materials and Atoms*.

600 Kuhlemann, J., Milivojević, M., Krumrei, I., Kubik, P., 2009. Last glaciation of the Šara Range
601 (Balkan peninsula): increasing dryness from the LGM to the Holocene. *Austrian Journal of*
602 *Earth Science* 102, 146-158.

603 Kuhlemann, J., Gachev, E., Gikov, A., Nedkov, S., Krumrei, I., Kubik, P., 2013. Glaciation in
604 the Rila mountains (Bulgaria) during the Last Glacial Maximum. *Quaternary International*
605 293, 51-62.

606 Lacey, J.H., Leng, M.J., Francke, A., Sloane, H.J., Milodowski, A., Vogel, H., Baumgarten,
607 H., Zanchetta, G., Wagner, B., 2016. Northern Mediterranean climate since the Middle
608 Pleistocene: a 637 ka stable isotope record from Lake Ohrid (Albania/Macedonia).
609 *Biogeosciences* 13, 1801-1820.

610 Leng, M.J., Wagner, B., Boehm, A., Panagiotopoulos, K., Vane, C.H., Snelling, A., Haidon,
611 C., Woodley, E., Vogel, H., Zanchetta, G., Baneschi, I., 2013. Understanding past climatic
612 and hydrological variability in the Mediterranean from Lake Prespa sediment isotope and
613 geochemical record over the Last Glacial cycle. *Quaternary Science Reviews* 66, 123-136.

614 Lézine, A.M., von Grafenstein, U., Andersen, N., Belmecheri, S., Bordon, A., Caron, B.,
615 Cazet, J.P., Erlenkeuser, H., Fouache, E., Grenier, C., Huntsman-Mapila, P., Hureau-
616 Mazaudier, D., Manelli, D., Mazaud, A., Robert, C., Sulpizio, R., Tiercelin, J.J., Zanchetta, G.,
617 Zeqollari, Z., 2010. Lake Ohrid, Albania, provides an exceptional multi-proxy record of
618 environmental changes during the last glacial–interglacial cycle. *Palaeogeography,*
619 *Palaeoclimatology, Palaeoecology* 287, 116-127.

620 Lifton, N., Sato, T., Dunai, T.J., 2014. Scaling in situ cosmogenic nuclide production rates
621 using analytical approximations to atmospheric cosmic-ray fluxes. *Earth and Planetary*
622 *Science Letters* 386, 149-160.

623 Lisiecki, L.E., Raymo, M.E., 2005. A Pliocene-Pleistocene stack of 57 globally distributed
624 benthic $\delta^{18}\text{O}$ records. *Paleoceanography* 20, PA1003.

625 Makos, M., Nitychoruk, J., Zreda, M., 2013. Deglaciation chronology and paleoclimate of the
626 Pięciu Stawów Polskich/Roztoki Valley, high Tatra Mountains, Western Carpathians, since
627 the Last Glacial Maximum, inferred from ^{36}Cl exposure dating and glacier–climate modelling.
628 *Quaternary International* 293, 63-78.

629 Marrero, S.M., Phillips, F.M., Caffee, M.W., Gosse, J.C., 2016. CRONUS-Earth cosmogenic
630 ^{36}Cl calibration. *Quaternary Geochronology* 31, 199-219.

631 Milivojević, M., Menković, L., Čalić, J., 2008. Pleistocene glacial relief of the central part of
632 Mt. Prokletije (Albanian Alps). *Quaternary International* 190, 112-122.

633 Panagiotopoulos, K., Aufgebauer, A., Schäbitz, F., Wagner, B., 2013. Vegetation and climate
634 history of the Lake Prespa region since the Lateglacial. *Quaternary International* 293, 157-
635 169.

636 Phillips, F.M., Zreda, M.G., Gosse, J.C., Klein, J., Evenson, E.B., Hall, R.D., Chadwick, O.A.,
637 Sharma, P., 1997. Cosmogenic ^{36}Cl and ^{10}Be ages of Quaternary glacial and fluvial
638 deposits of the Wind River Range, Wyoming. *Geological Society of America Bulletin* 109,
639 1453-1463.

640 Plan, L., 2005. Factors controlling carbonate dissolution rates quantified in a field test in the
641 Austrian alps. *Geomorphology* 68, 201-212.

642 Popovska, C., Bonacci, O., 2007. Basic data on the hydrology of Lakes Ohrid and Prespa.
643 *Hydrological Processes* 21, 658-664.

644 Putkonen, J., Swanson, T., 2003. Accuracy of cosmogenic ages for moraines. *Quaternary*
645 *Research* 59, 255-261.

646 Reuther, A.U., Urdea, P., Geiger, C., Ivy-Ochs, S., Niller, H.-P., Kubik, P.W., Heine, K., 2007.
647 Late Pleistocene glacial chronology of the Pietrele Valley, Retezat Mountains, Southern
648 Carpathians constrained by ^{10}Be exposure ages and pedological investigations. *Quaternary*
649 *International* 164-165, 151-169.

650 Ribolini, A., Isola, I., Zanchetta, G., Bini, M., Sulpizio, R., 2011. Glacial features on the
651 Galicica Mountains, Macedonia: Preliminary Report. *Geogr. Fis. Dinam. Quat.* 34, 247-255.

652 Sarikaya, M.A., Çiner, A., Haybat, H., Zreda, M., 2014. An early advance of glaciers on
653 Mount Akdağ, SW Turkey, before the global Last Glacial Maximum; insights from
654 cosmogenic nuclides and glacier modeling. *Quaternary Science Reviews* 88, 96-109.

655 Schimmelpfennig, I., Benedetti, L., Garreta, V., Pik, R., Blard, P.-H., Burnard, P., Bourlès, D.,
656 Finkel, R., Ammon, K., Dunai, T., 2011. Calibration of cosmogenic ^{36}Cl production rates
657 from Ca and K spallation in lava flows from Mt. Etna (38°N , Italy) and Payun Matru (36°S ,
658 Argentina). *Geochimica et Cosmochimica Acta* 75, 2611-2632.

659 Sharma, P., Kubik, P., Fehn, U., Gove, H.E., Nishiizumi, K., Elmore, D., 1990. Development
660 of ^{36}Cl standards for AMS. *Nuclear Instruments and Methods in Physics Research B52*,
661 410-415.

662 Stephenson, W.J., Finlayson, B.L., 2009. Measuring erosion with the micro-erosion meter—
663 Contributions to understanding landform evolution. *Earth-Science Reviews* 95, 53-62.

664 Stone, J.O., Allan, G.L., Fifield, L.K., Cresswell, R.G., 1996. Cosmogenic chlorine-36 from
665 calcium spallation. *Geochimica et Cosmochimica Acta* 60, 679-692.

666 Vogel, H., Wagner, B., Zanchetta, G., Sulpizio, R., Rosén, P., 2010a. A paleoclimate record
667 with tephrochronological age control for the last glacial-interglacial cycle from Lake Ohrid,
668 Albania and Macedonia. *Journal of Paleolimnology* 44, 295-310.

669 Vogel, H., Zanchetta, G., Sulpizio, R., Wagner, B., Nowaczyk, N., 2010b. A
670 tephrostratigraphic record for the last glacial-interglacial cycle from Lake Ohrid, Albania and
671 Macedonia. *Journal of Quaternary Science* 25, 320-338.

672 Wagner, B., Reicherter, K., Daut, G., Wessels, M., Matzinger, A., Schwalb, A., Spirkovski, Z.,
673 Sanxhaku, M., 2008. The potential of Lake Ohrid for long-term palaeoenvironmental
674 reconstructions. *Palaeogeography, Palaeoclimatology, Palaeoecology* 259, 341-356.

675 Wagner, B., Vogel, H., Zanchetta, G., Sulpizio, R., 2010. Environmental change within the
676 Balkan region during the past ca. 50 ka recorded in the sediments from lakes Prespa and
677 Ohrid. *Biogeosciences* 7, 3187-3198.

678 Watzin, M.C., Puka, V., Naumoski, T.B., 2002. Lake Ohrid and its Watershed, State of the
679 Environment Report. Lake Ohrid Conservation Project. Tirana, Albania and Ohrid,
680 Macedonia.

681 Žebre, M., Stepišnik, U., 2014. Reconstruction of Late Pleistocene glaciers on Mount Lovćen,
682 Montenegro. *Quaternary International* 353, 225-235.

683

684

685

686

687

688

689

690 Figure 1: A) Overview map with Macedonia highlighted B) Overview map with locations of
691 the Galicica Mountains, Lake Ohrid, Lake Prespa and Lake Maliq, Asterisks mark the City of
692 Ohrid and Resen, respectively, where climate stations are situated C) Digital surface model
693 (DSM) of the cirque with the G4 moraine series. The model was created using structure-
694 from-motion photogrammetry with the software Agisoft Photoscan. (please print as colored
695 image)

696

697 Figure 2: Geomorphological overview map of the two cirques beneath Magaro Mountain.
698 Sampled moraine is highlighted in detail map (modified after Ribolini et al., 2011). (please
699 print as colored image)

700

701 Figure 3: Panorama picture of the sampled moraine. Arrows indicate position of sampled
702 boulders. Picture is taken in downvalley direction, i.e. picture shows inner side of the
703 moraine. (please print as colored image)

704

705 Figure 4: Sampled boulders on the moraine crest. Arrows point to exact sampling position on
706 each boulder. Hammer for scale. (please print as colored image)

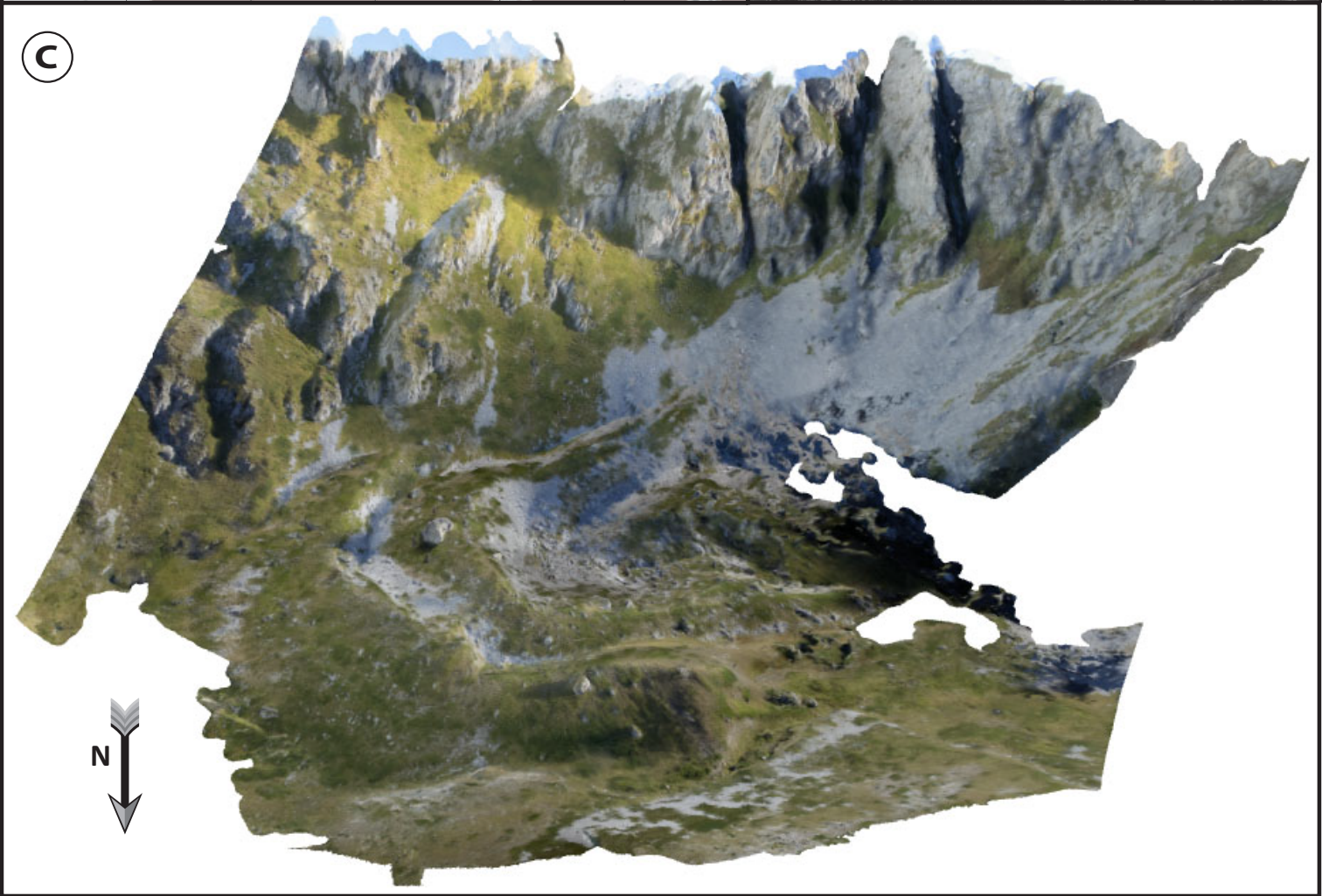
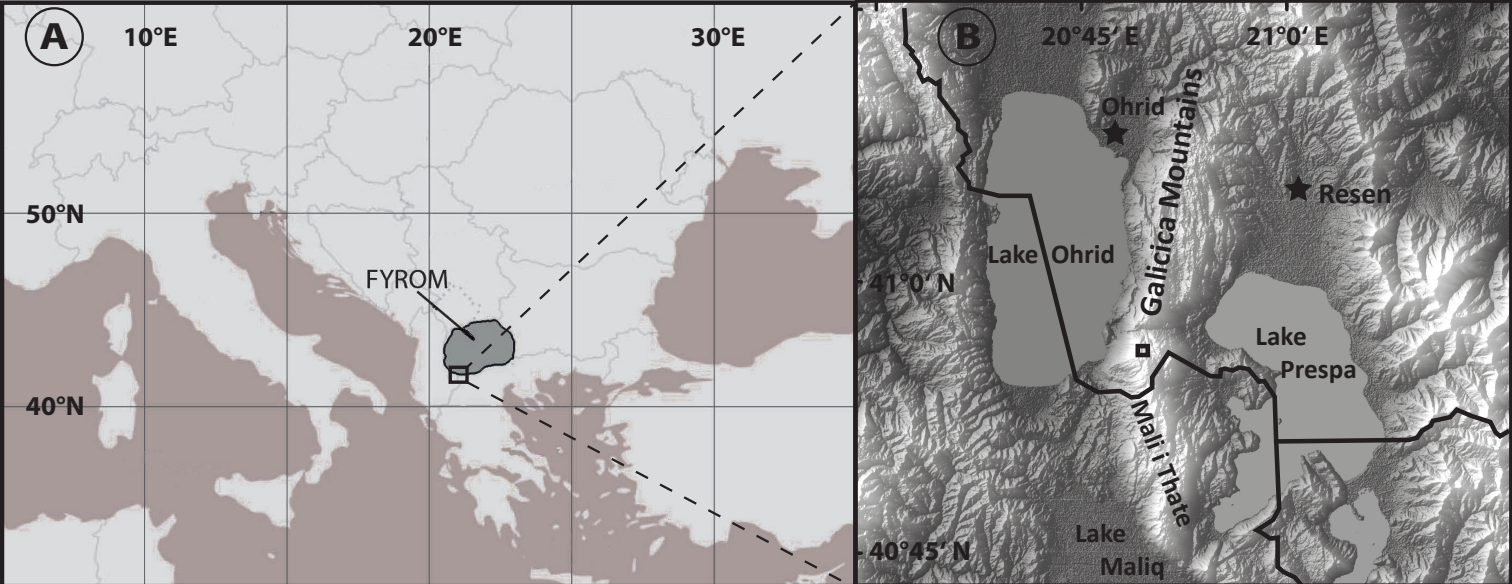
707

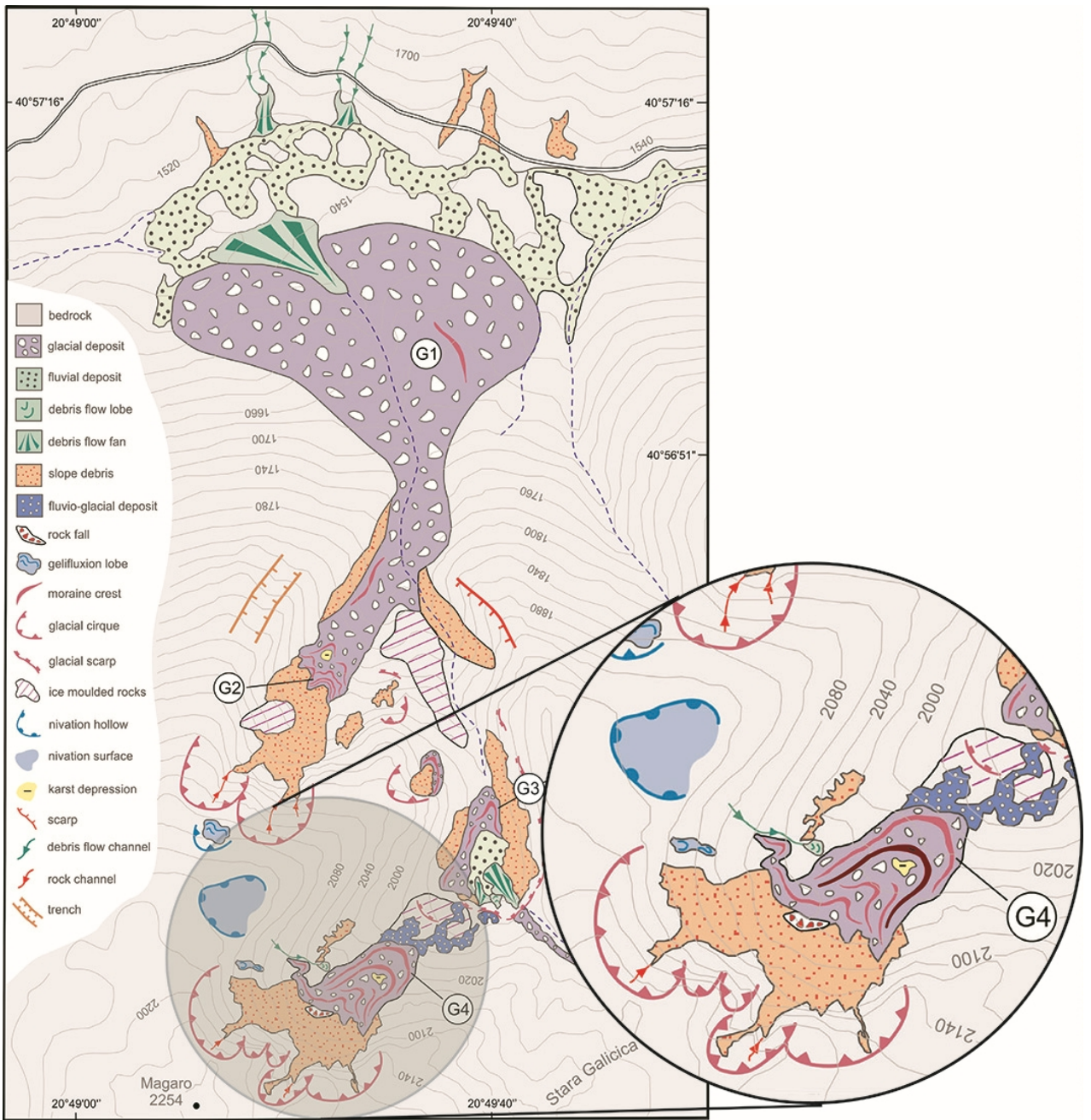
708 Figure 5: Probability density plots showing the calculated ages. The dashed box reflects the
709 period of the Younger Dryas, blue area the Last Glacial Maximum. Black lines represent
710 normal distribution of the single ages, red line displays cumulative relative probability.
711 Corrections for erosion and snow cover are given in the diagrams, respectively. Thick arrows
712 indicate significant impact of the applied correction on the exposure ages, while thin arrow
713 indicates only minor impact. We used a production rate of ^{36}Cl from Ca spallation of 56 at g^{-1}
714 a^{-1} (Marrero et al., 2016) and LSD scaling. (please print as colored image)

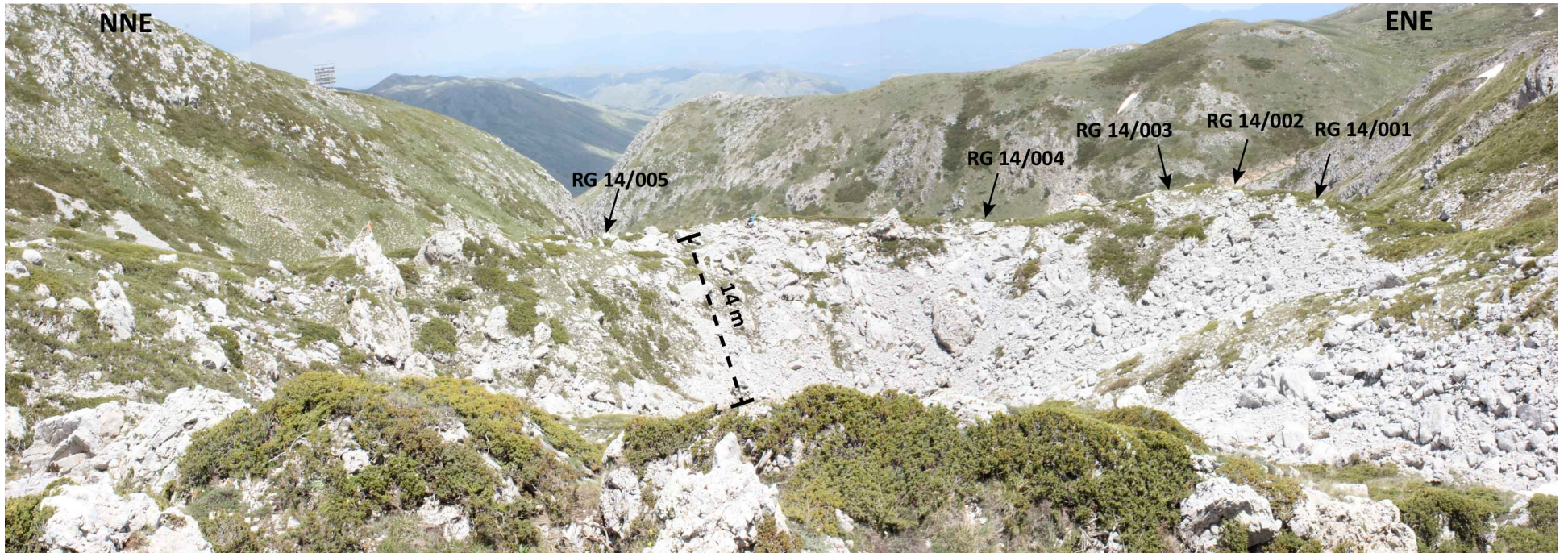
715

716 Figure 6: Overview map with locations of studied glaciers on the Balkan Peninsula: 1)
717 Durmitor Massif 2) Mt. Orjen 3) Mt. Lovćen 4) Mt. Prokletije 5) Rila Mts. 6) Mt. Tymphi 7) Mt
718 Smolikas 8) Galicica Mts. 9) Šara Mts. Lake Dojran is marked with the red asterisk. Authors
719 corresponding to the Study areas are noted in the text. (please print as colored image)

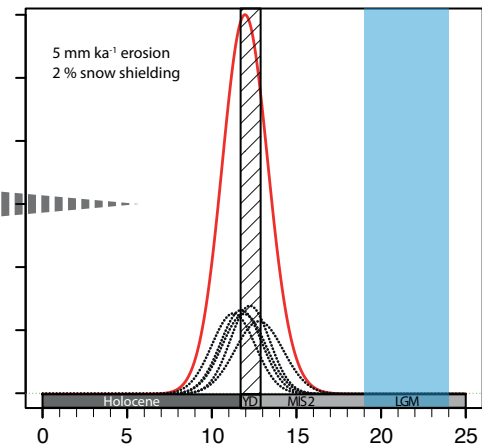
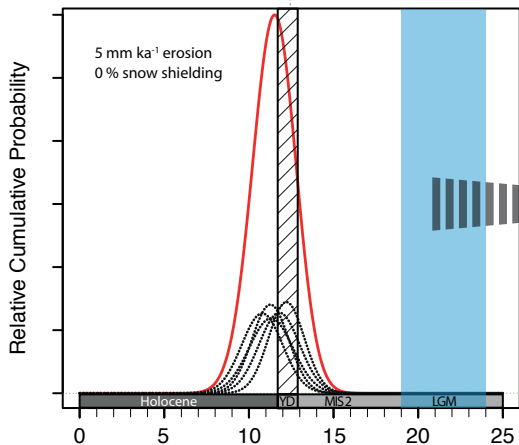
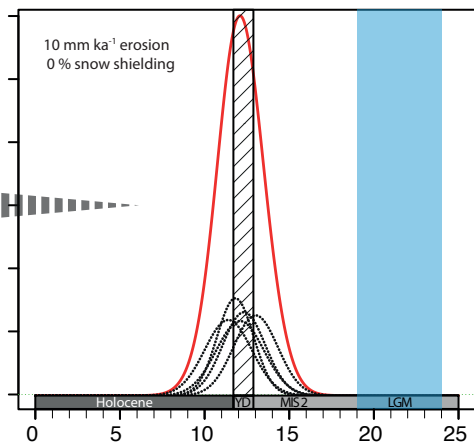
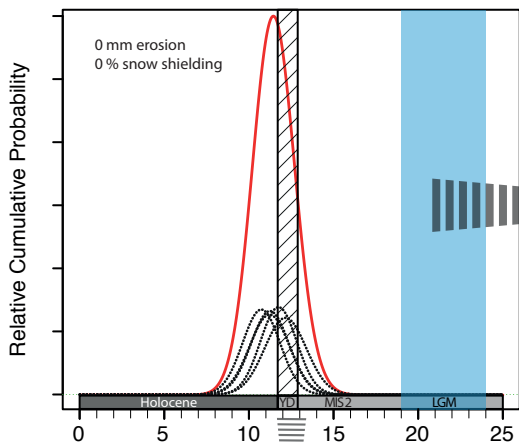
720











Cosmogenic Exposure Ages (ka)

Cosmogenic Exposure Ages (ka)

